

Connection between parsec-scale radio jet and gamma-ray flares in the blazar 1156+295

V. Ramakrishnan^{*,1} J. León-Tavares^{2,3} E. A. Rastorgueva-Foi^{1,4} K. Wiik⁵
S. G. Jorstad^{6,7} A. P. Marscher⁶ M. Tornikoski¹ I. Agudo^{8,9,6} A. Lähteenmäki^{1,10}
E. Valtaoja⁵ M. F. Aller¹¹ D. A. Blinov^{12,7} C. Casadio⁹ N. V. Efimova^{7,13}
M. A. Gurwell¹⁴ J. L. Gómez⁹ V. A. Hagen-Thorn⁷ M. Joshi⁶ E. Järvelä^{1,10}
T. S. Konstantinova⁷ E. N. Kopatskaya⁷ V. M. Larionov^{7,13} E. G. Larionova⁷
L. V. Larionova⁷ N. Lavonen¹ N. R. MacDonald⁶ I. M. McHardy¹⁵ S. N. Molina⁹
D. A. Morozova⁷ E. Nieppola^{1,3} J. Tammi¹ B. W. Taylor^{6,16} and I. S. Troitsky⁷

¹Aalto University Metsähovi Radio Observatory, Finland

²Instituto Nacional de Astrofísica Óptica y Electrónica (INAOE), México

³Finnish Centre for Astronomy with ESO (FINCA), University of Turku, Finland

⁴School of Mathematics and Physics, University of Tasmania, Australia

⁵Tuorla Observatory, Department of Physics and Astronomy, University of Turku, Finland

⁶Institute for Astrophysical Research, Boston University, USA

⁷Astronomical Institute, St. Petersburg State University, Russia

⁸Joint Institute for VLBI in Europe, the Netherlands

⁹Instituto de Astrofísica de Andalucía, CSIC, Spain

¹⁰Aalto University Department of Radio Science and Engineering, Finland

¹¹University of Michigan, Astronomy Department, USA

¹²Department of Physics and Institute of Theoretical & Computational Physics, University of Crete, Greece

¹³Pulkovo Observatory, Russia

¹⁴Harvard-Smithsonian Center for Astrophysics, USA

¹⁵Department of Physics and Astronomy, University of Southampton, UK

¹⁶Lowell Observatory, USA

E-mail: venkatessh.ramakrishnan@aalto.fi

We discuss the connection of γ -ray events to the superluminal component ejection in the jet of the blazar 1156+295. The broadband variability of the source is analysed using multifrequency observations (X-ray through mm single-dish) and radio band imaging data at 43 GHz from Very Long Baseline Array (VLBA) observations. The kinematics of the jet over the interval 2007.0–2012.5, reveal the presence of four moving and one stationary component in the inner region of the blazar jet. The propagation of the third and fourth components in the jet corresponds closely in time to the active phase of the source in γ rays. The physical signatures of these components allowed us to constrain the γ -ray emitting region in the parsec-scale jet.

12th European VLBI Network Symposium and Users Meeting

7-10 October 2014

Cagliari, Italy

*Speaker.

1. Introduction

Blazars are a subclass of active galactic nuclei (AGN) with a relativistic jet oriented close to the line of sight, which causes Doppler boosting of the jet emission and leads to strong variability at all wavebands from radio to γ rays. It is generally accepted that the low energy emission (from radio to UV or, in some cases, X-rays) is generated via synchrotron radiation by relativistic electrons in the jet plasma, while high-energy emission (from X-ray to γ rays) is the result of inverse Compton scattering of seed photons by the same population of relativistic electrons. The seed photons could be either synchrotron photons generated in the jet [synchrotron self-Compton model; e.g., 5] or ambient photons [external Compton model; 18]. Several models have been proposed regarding the location of the γ -ray emission site relative to the central engine in blazars. Some of them constrain the location closer to the supermassive black hole (< 0.1 – 1 pc), where the seed photons originate from the broad-line region (BLR) or the accretion disk [e.g., 7, 18]. On the other hand, results from multifrequency studies suggest that the region where the bulk of the γ rays is produced is usually located downstream of the canonical BLR [e.g., 14, 15, 16].

The blazar 1156+295, located at redshift $z = 0.729$, displays strong variability across the electromagnetic spectrum. The Large Area Telescope on board the *Fermi Gamma-ray Space Telescope* (hereafter *Fermi/LAT*) detected the source at a flux level of 1.6×10^{-7} photons $\text{cm}^{-2} \text{s}^{-1}$ just after three months of operation [1]. To study the flaring behaviour of the source and to determine the location of the γ -ray emission region, we perform a multifrequency analysis.

2. Observations and data reduction

We obtained 0.1–200 GeV γ -ray fluxes by analyzing the *Fermi/LAT* data for the interval, 2008 August 4 to 2011 December 31 using the *Fermi* Science Tools version v9r33p0. To assure a high quality selection of the data, an event class of 2 was applied with a further selection of zenith angle $> 100^\circ$ to avoid contamination from photons coming from the Earth's limb. The photons were extracted from a circular region centred on the source, within a radius of 15° . Our final fluxes were obtained using an unbinned likelihood methodology from 7-day integrations. We modelled our source using a simple power-law.

In the X-rays, we obtained the *Swift* X-ray Telescope (XRT) data over the energy range, 0.3–10 keV, from an ongoing monitoring programme of *Fermi/LAT* monitored sources. The *Swift*/XRT data reduction method is discussed in Williamson et al. [20]. At optical wavelengths, we obtained *B*-, *V*-, *R*- and *I*-band data from an ongoing monitoring programme of blazars at the following optical facilities: Catalina Real-time Transient Survey [6]¹, Lowell Observatory (1.83-m Perkins Telescope equipped with the PRISM camera), Calar Alto (2.2-m Telescope, observations under the MAPCAT² programme), Liverpool 2-m Telescope, Crimean Astrophysical Observatory (0.7-m Telescope), and St. Petersburg State University (0.4-m Telescope). The optical data analysis procedures except for the Catalina data, were performed as discussed in Jorstad et al. [10].

¹<http://crts.caltech.edu/>

²<http://www.iaa.es/~iagudo/research/MAPCAT>

At millimetre wavelengths, we obtained the data at 230 GHz (1.3 mm) from the Submillimeter Array³ (SMA) and 37 GHz (8 mm) single-dish fluxes from Aalto University Metsähovi Radio Observatory. Refer Gurwell et al. [9] (SMA) and Teräsraanta et al. [19] (Metsähovi) for data reduction methods. To investigate the kinematics of the inner regions of the jet, we used 47 VLBA observations at 43 GHz from the Boston University blazar monitoring programme⁴. The data reduction and calibration was performed as discussed in Jorstad et al. [11]. We then modelled the complex visibility data with multiple components using the task *modelfit* in the DIFMAP program, with each represented by a circular Gaussian brightness distribution.

3. Discussion

The blazar 1156+295 was active for more than 3 months (from flare B to C in Figure 1) in γ rays before returning to a quiescent state. Flare B, with a peak flux of 1.4×10^{-6} photons $\text{cm}^{-2} \text{s}^{-1}$, is the brightest event observed in the γ -ray light curve. In the optical wavebands, the source was flaring roughly on a yearly basis, but owing to the gaps due to solar conjuncture the data was not much useful to the analysis. At mm wavelengths, the source exhibited two characteristic exponential flares.

The kinematics of the inner region in the jet of the blazar 1156+295, based on the 43 GHz VLBA observations, reveal the presence of four moving, and one stationary, components (Figure 2). We find that the properties of the moving components differ from one another (see Table 1). According to Figure 1, the ejection of C3 and C4 corresponds to the beginning of strong γ -ray activity. Component C4 can be classified as a trailing component, forming in the wake of the leading component, C3. After propagating over ~ 0.2 mas, C4 accelerates (Figure 2), increasing the apparent speed to $23.2c$. This behaviour is in accordance with the simulation by Agudo et al. [2], who find that the trailing components represent pinch waves excited by the main disturbance, so that an increase of their speed at larger distance reflects acceleration of the expanding jet. Under this scenario, the split of C4 from C3 towards the end of 2010 coincides with γ -ray flare C.

Table 1: Measured physical parameters of the components within 0.5 mas of the radio core.

ID	Number of Epochs	μ (mas yr ⁻¹)	β_{app} (c)	t_o (yr)	Δt_{var} (yr)	δ_{var}	Γ_{var}	θ_{var} ($^\circ$)
(1)	(2)	(3)	(4)	(5)	(6)	(7)	(8)	(9)
C1	6	0.147 ± 0.02	6.18 ± 0.8	2006.53 ± 0.12	0.75	10.85 ± 1.5	7.23 ± 1.4	4.56 ± 0.3
C2	10	0.278 ± 0.01	11.69 ± 1.5	2008.74 ± 0.06	0.44	18.54 ± 2.3	12.98 ± 2.1	2.79 ± 0.4
C3	9	0.137 ± 0.005	5.76 ± 0.4	2010.12 ± 0.05	1.06	7.9 ± 0.3	6.13 ± 1.2	6.83 ± 0.4
C4 ^a	7	0.142 ± 0.05	5.97 ± 0.8	2010.31 ± 0.08	0.55	15.37 ± 1.7	8.8 ± 0.5	2.52 ± 0.2
C4 ^b	6	0.552 ± 0.08	23.22 ± 2.3	$\sim 2011.4^c$	0.24	45.95 ± 2.1	28.85 ± 1.4	1 ± 0.08

Columns are as follows: (1) component number, (2) number of epochs over which a component was identified, (3) proper motion, (4) apparent speed, (5) ejection epoch of the component, (6) variability timescale, (7)(8)(9) - variability Doppler factor, Lorentz factor and viewing angle.

^a estimates obtained before acceleration

^b estimates obtained after acceleration

^c time of acceleration

³<http://sma1.sma.hawaii.edu/callist/callist.html>

⁴<http://www.bu.edu/blazars/VLBAproject.html>

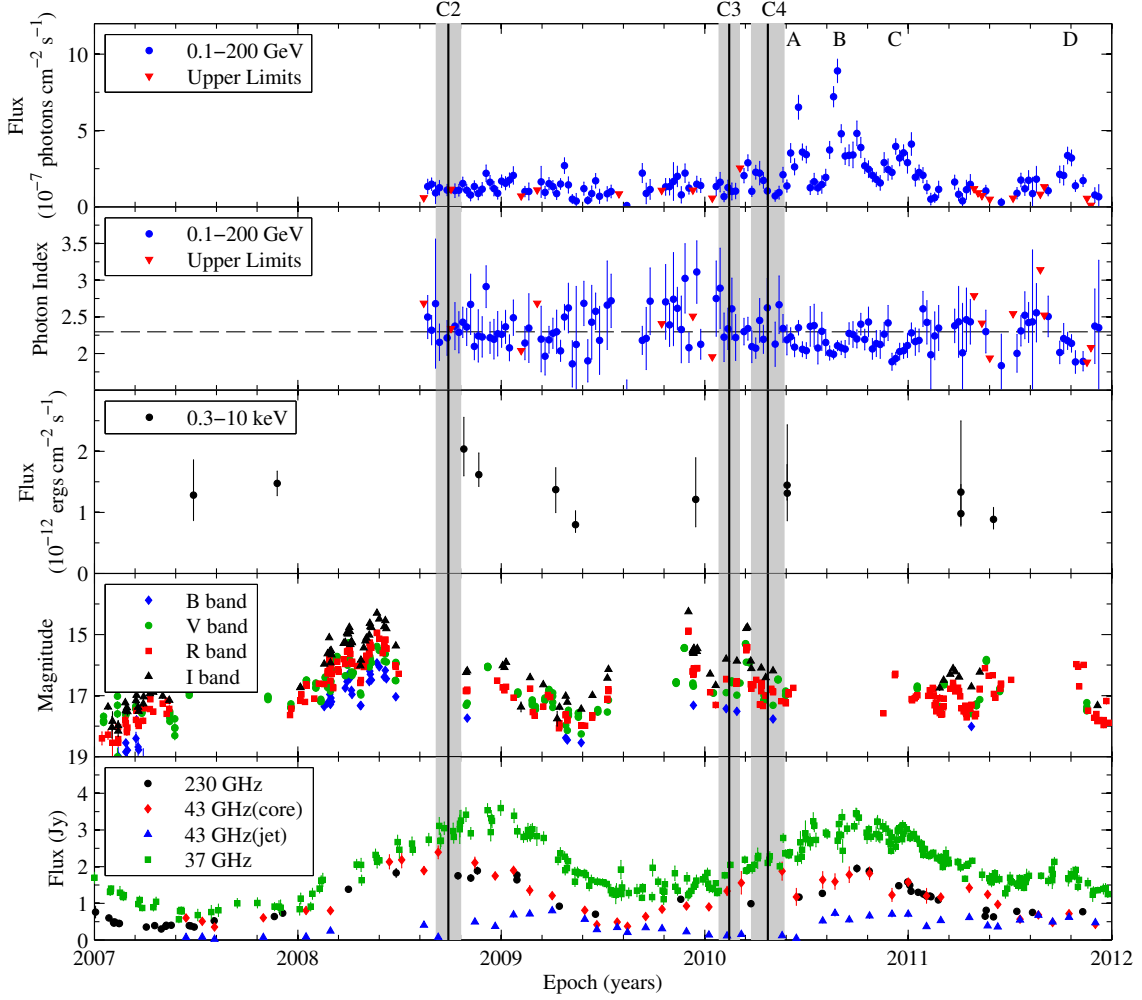


Figure 1: Light curves of 1156+295 from 2007 through 2011. From the top: (1) weekly binned γ -ray flux from *Fermi*/LAT at 0.1–200 GeV; 2σ upper limits are denoted as inverted red triangles. (2) Photon Index of the weekly binned γ -ray light curve; the dashed line represents the 2FGL photon index estimate. (3) *Swift*/XRT X-ray flux at 0.3–10 keV. (4) Optical data at various bands. The gaps in the optical data are due to solar conjunction. (5) Variations at mm wavelengths in bottom panel. The vertical lines are the ejection epochs of the components C2 (2008.74), C3 (2010.12) and C4 (2010.31) obtained from the VLBA data with their 1σ uncertainties denoted by the corresponding shaded interval.

The flux density evolution of the component C4 shows considerable variability which could be explained in terms of interaction with a stationary component [e.g., 8, 13], or by an increase in the Doppler boosting of the component at the positions where it is closer to the line of sight while travelling along a helical jet [e.g., 4]. Although helicity has been studied in detail in this source [21], from Figure 2, the possibility of the interaction of C4 with S1 can be established. Component C4, after being accelerated around 2011.3, interacts with stationary component S1 (formed by early 2010) at 0.4 ± 0.04 mas around 2011.5. Sub-flare D in the γ rays occur ~ 2 months after this interaction, which places the location of the sub-flare $\gtrsim 4$ pc (projected) from the radio core. During the interaction of C4 with S1, there is also an increase in the flux of C4. The stationary

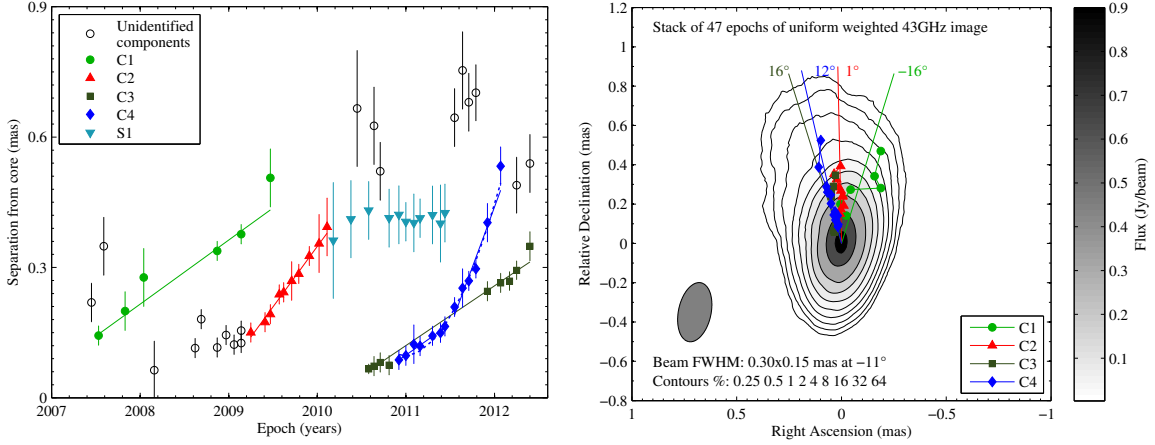


Figure 2: Left: Component separation from the 43 GHz radio core versus time. Four moving components (C1, C2, C3 and C4) and one stationary component (S1) are identified in the jet. The solid lines indicate motion with no acceleration, while the dotted lines indicate accelerated motion fits. Right: Uniformly weighted stacked VLBA image of 1156+295. The contour levels and beam size are mentioned in the figure. Various components' average position angles are denoted by the solid line with the average mentioned.

feature could be produced at a bend in the jet, since this might also explain the observed position angle swing (right panel of Figure 2).

The distance to the radio core from the black hole at 15 GHz is ~ 30 pc [17], well beyond the canonical BLR. Although the radio core at 43 GHz should be a factor ~ 3 closer to the black hole, this still places it well beyond the inner parsec where the BLR is expected to be located. The latter, in combination with our main finding that the γ -ray flare is produced after ~ 2 months of the start of component ejection, would allow us to rule out the model where the most intense γ rays are produced by upscattering of photons from the BLR. However, recent results by León-Tavares et al. [12] indicate that, in the quasar 3C 454.3, emission-line clouds can exist (and be ionized) at distances of several parsecs down the jet. This in turn suggests that IC scattering of line photons can even occur at distances well beyond the inner parsec.

No significant γ -ray event was found during the first mm flare, whereas the second mm flare was accompanied by strong γ -ray activity. The radiative transfer modelling of the source by Aller et al. [3] for the interval when the source was active in the γ rays, suggests that substantial part of the magnetic field energy density lies in an ordered component oriented along the jet axis from modelling the radio flare using 4 shocks. This implies that the γ rays and the radio might be unrelated during the first mm flare. However, it is possible that a γ -ray flare could have occurred in 2008 prior to the start of the *Fermi* observations.

4. Conclusion

The blazar 1156+295 exhibited one major flare and three sub-flares in 2010 and towards the end of 2011. From the 43 GHz VLBI maps, we identify 4 moving and 1 stationary component. The mm- γ -ray connection in the source can be explained by the complex changes in the parsec-scale structure of the jet from the perspective of trailing shocks. There is also evidence suggesting that

the bulk of γ rays was produced downstream of the radio core. This conclusion is suggested by the coincidence of sub-flare D in the γ rays and the component interaction.

VR acknowledges RadioNet3 for financial support to participate in the 12th European VLBI Network Symposium & Users Meeting.

References

- [1] Abdo, A. A., Ackermann, M., Ajello, M., et al. 2009, *ApJ*, 700, 597
- [2] Agudo, I., Gómez, J. L., Martí, J. M., et al. 2001, *ApJ*, 549, L183
- [3] Aller, M. F., et al. 2014, *ApJ*, 791, 93
- [4] Aloy, M. Á., Martí, J. M., Gómez, J. L., et al. 2003, *ApJ*, 585, L109
- [5] Atayan, A. M., & Nahapetian, A. 1989, *A&A*, 219, 53
- [6] Drake, A. J., Djorgovski, S. G., Mahabal, A., et al. 2009, *ApJ*, 696, 870
- [7] Foschini, L., Ghisellini, G., Tavecchio, F., Bonnoli, G., & Stamerra, A. 2011, *A&A*, 530, A77
- [8] Gómez, J. L., Martí, J. M., Marscher, A. P., Ibáñez, J. M., & Alberdi, A. 1997, *ApJ*, 482, L33
- [9] Gurwell, M. A., Peck, A. B., Hostler, S. R., Darrah, M. R., & Katz, C. A. 2007, *From Z-Machines to ALMA: (Sub)Millimeter Spectroscopy of Galaxies*, 375, 234
- [10] Jorstad, S. G., Marscher, A. P., Larionov, V. M., et al. 2010, *ApJ*, 715, 362
- [11] Jorstad, S. G., Marscher, A. P., Lister, M. L., et al. 2005, *AJ*, 130, 1418
- [12] León-Tavares, J., Chavushyan, V., Patiño-Álvarez, V., et al. 2013, *ApJ*, 763, L36
- [13] León-Tavares, J., Lobanov, A. P., Chavushyan, V. H., et al. 2010, *ApJ*, 715, 355
- [14] León-Tavares, J., Valtaoja, E., Giommi, P., et al. 2012, *ApJ*, 754, 23
- [15] León-Tavares, J., Valtaoja, E., Tornikoski, M., Lähteenmäki, A., & Nieppola, E. 2011, *A&A*, 532, A146
- [16] Marscher, A. P., Jorstad, S. G., Larionov, V. M., et al. 2010, *ApJ*, 710, L126
- [17] Pushkarev, A. B., Hovatta, T., Kovalev, Y. Y., et al. 2012a, *A&A*, 545, A113
- [18] Tavecchio, F., Ghisellini, G., Bonnoli, G., & Ghirlanda, G. 2010, *MNRAS*, 405, L94
- [19] Teräsranta, H., Tornikoski, M., Mujunen, A., et al. 1998, *A&AS*, 132, 305
- [20] Williamson, K. E., Jorstad, S. G., Marscher, A. P., et al. 2014, *ApJ*, 789, 135
- [21] Zhao, W., Hong, X.-Y., An, T., et al. 2011, *A&A*, 529, A113